

Optical Imaging and Spectroscopic Observation of the Galactic Supernova Remnant G85.9-0.6

F.Gök¹ , A.Sezer^{2,4} , E.Aktekin¹, T.Güver³ and N.Ercan⁴

Akdeniz University, Faculty of Art and Sciences, Department of Physics

Antalya, 07058, Turkey

TÜBİTAK Space Technologies Research Institute, Middle-East Technical University, 06531

Ankara, Turkey

University of Arizona, Department of Astronomy, 933 N. Cherry Ave., Tucson, AZ, 85721

Boğaziçi University, Faculty of Art and Sciences, Department of Physics

İstanbul, 34342, Turkey

Received _____; accepted _____

Not to appear in Nonlearned J., 45.

ABSTRACT

Optical CCD imaging with $H\alpha$ and [SII] filters and spectroscopic observations of the galactic supernova remnant G85.9-0.6 have been performed for the first time. The CCD image data are taken with the 1.5m Russian-Turkish Telescope (RTT150) at TÜBİTAK National Observatory (TUG) and spectral data are taken with the Bok 2.3 m telescope on Kitt Peak, AZ.

The images are taken with narrow-band interference filters $H\alpha$, [SII] and their continuum. [SII]/ $H\alpha$ ratio image is performed. The ratio obtained from [SII]/ $H\alpha$ is found to be ~ 0.42 , indicating that the remnant interacts with HII regions. G85.9-0.6 shows diffuse-shell morphology. [SII] $\lambda\lambda 6716/6731$ average flux ratio is calculated from the spectra, and the electron density N_e is obtained to be 395 cm^{-3} . From [OIII]/ $H\beta$ ratio, shock velocity has been estimated, pre-shock density of $n_c = 14 \text{ cm}^{-3}$, explosion energy of $E = 9.2 \times 10^{50}$ ergs, interstellar extinction of $E(B-V) = 0.28$, and neutral hydrogen column density of $N(HI) = 1.53 \times 10^{21} \text{ cm}^{-2}$ are reported.

Subject headings: G85.9-0.6; optical observation; CCD image; spectra

1. Introduction

Galactic supernova remnants (SNRs) are now as many as 274 (Green 2009). Most of them are observed in radio wavelengths from their non-thermal synchrotron emission despite their very few optical observations. The reason for this is because of the dust and gas around the galactic disk stopping the optical light coming from them. However, only recently optical observations of SNRs can be performed by using narrow-band interference filters and providing rather long posing intervals (e.g. Fesen et al. 1997, 2008; Mavromataki et al. 2001; Mavromataki 2003; Boumis et al. 2002, 2009; Gök et al. 2008). Recently, X-ray satellites like Chandra, XMM-Newton, Suzaku observed some SNRs in X-ray band (e.g. Bamba et al. 2000; Katsuda et al. 2009).

The galactic supernova remnant G85.9-0.6 ($\alpha = 20^h58^m40^s$, $\delta = 44^{\circ}53'$) was discovered in the Canadian Galactic Plane Survey (CGPS) (Kothés et al. 2001). G85.9-0.6 has a radio surface brightness at 1 GHz of $2 \times 10^{-22} \text{ Wattm}^{-2} \text{ Hz}^{-1} \text{ sr}^{-1}$. Kothés et al. (2001) has detected no HI features corresponding to the SNR. This and the low radio and X-ray brightness, suggest expansion in a low-density medium. The SNR may lie in the low-density region between the local and Perseus spiral arms, at a distance of about 5 kpc. The most likely event that would produce an SNR in such a low density medium might be a Type Ia supernova. It has a radius of $\sim 12'$ (Kothés et al. 2001). G85.9-0.6 has a diffuse type structure in X-ray region, where its electron density is 0.20 cm^{-3} and the ejecta mass is at order of $1.0 M_{\odot}$ (Jackson et al. 2008).

[SII]/H α ratio is an important criteria to distinguish HII regions and SNRs (Mathewson & Clarke 1972; Dopita 1997). In HII regions most sulphur atoms are in the form of SIII, since there is a strong photo-ionization and [SII]/H α ratio is expected to be in the range of $\sim 0.1 - 0.3$ (Osterbrock 1989), however recent models give this range to be 0.1-0.5 (Dopita et al. 2000; Kewley et al. 2001), for SNRs on the other hand, it is 0.5-1.0

(Raymond 1979; Shull & McKee 1979).

In this work, we selected the SNRs (G16.2-2.7, G17.8-2.6, G36.6+2.6, G83.0-0.3 and G85.9-0.6) that have no optical observation in literature so far and have proper coordinates to observe at TUG. We take their $H\alpha$ images with 300 seconds exposure time.

Theoretical models predict that, in SNRs, the temperature of the regions that give optical emission should be at $\sim 10^4 K$, therefore, the intensity of $H\alpha$ emission line should be larger compared to the other emission lines. For this reason, $H\alpha$ interference filters are preferred for determining SNRs (Osterbrock 1989). With $H\alpha$ filter we found radiation only from G85.9-0.6 and studied its optical image and spectrum. The observations and results are presented in sections 2. and 3., respectively. In the last part we discuss the results.

2. Observations

2.1. Imaging

The CCD images of G85.9-0.6 are obtained with the 1.5m RTT150 at TUG, Antalya, Türkiye. The data are taken with a 2048×2048 pixel CCD447, with a pixel size of $15\mu m$ resulting in a $13.5 \text{ arcmin} \times 13.5 \text{ arcmin}$ field of view, with a plate scale of $0''.39 \text{ pixel}^{-1}$. Images are obtained with $H\alpha$, [SII] and their continuum filters within 900 seconds exposure times. Continuum filters are used to eliminate contamination from background starlight. Bias frames and dome flats are also observed for data reduction. The observations and interference filter characteristics are given in Table 1. The coordinates quoted in this work refer to epoch 2000. The image reduction is performed by using standard IRAF (Image Reduction Analysis Facility) routines.

Backgrounded, flat-fielded, trimmed and continuum subtracted [SII] and $H\alpha$ images are prepared. In Figure 1, $H\alpha$, $H\alpha$ cont., $H\alpha$ - $H\alpha$ cont. and [SII], [SII] cont., [SII]-[SII] cont.

images are presented. The images have been smoothed to suppress the remaining of the imperfect continuum subtraction.

2.2. Spectroscopy

An optical spectrum of SNR G85.9-0.6, covering 3750 - 7250 Å range, was obtained on UT 2009 June 16 at the Bok 2.3 m telescope on Kitt Peak, AZ, using the Boller and Chivens Spectrograph at the Richey-Chretien f/ 9 focus together with a thinned back-illuminated 1200×800, 15μm pixel Loral CCD. We used a 1st order 400 g/mm grating blazed at 4889 Å. With a slit width of 2.5 arcseconds a typical resolution of 6 Å was achieved at a reciprocal dispersion of 2.78 Å / pix on the CCD. Spectrums are taken on the image from three different intensive emission regions far from the stars. The coordinates of these regions and exposure times are listed in Table 2.

The data reduction is carried out by using the standard IRAF routines. Each frame is bias subtracted and for flat- field correction halogen lamps are used. Then with *apall* package under *noao.twodspec.apextract*, each spectrum is cleaned from external factors like sky and cosmic rays. The *apall* package selects an aperture for the target spectrum, and two apertures for the sky spectrum. The apertures for the sky spectrum are selected a dozen or so pixels, not illuminated by the object, above and below the target spectrum. *Apall* takes the average of the two sky spectrum and subtracts it from the target spectrum giving a sky subtracted target spectrum. *Identify*, *reidentify*, *hedit* and *dispcor* packages under *noao.onedspec* are used for wavelength calibration. For flux calibration, *sensfunc* package under *noao.onedspec* and *calibrate* package under *noao.twodspec.longslit* are used as described by Massey (1997). The spectra is dereddened by using *dereddened* task under *noao.onedspec*. The spectrophotometric standard star HR5501 is observed for flux calibration of the spectra (Hamuy et al. 1992). For wavelength calibration, however,

helium-neon (He-Ne) arc lamps are used.

The spectra obtained for three region are shown in Figure 2. In the optical spectra of SNRs; $H\alpha$, $H\beta$ and $[OIII]\lambda 4959, \lambda 5007$, $[NII]\lambda 6548, \lambda 6584$, $[SII]\lambda 6716, \lambda 6731$ known as forbidden lines, are expected. Taking the temperature $10^4 K$ which is convenient for optical radiation, the density of the medium, the energy of the supernova explosion, interstellar absorption, neutral Hydrogen column density, shock wave velocities and all other related physical parameters are derived from these lines.

3. Results

In Figure 3, we present $[SII]-[SII]_{cont.}/H\alpha-H\alpha_{cont.}$ image of the remnant G85.9-0.6. Continuum subtraction and image division are done with IRAF *imarith* package. *Imarith* package subtracts and divides the number of photons in each pixel of the image obtained with the above mentioned filters. Calculated $[SII]/H\alpha$ ratios and their errors in parenthesis taken from 10 different regions on the image are listed in Table 3, the average of these ratios is 0.42 ± 0.04 .

Figure 4 presents the correlation between $H\alpha$ emission and the radio emission of G85.9-0.6 at 1.4 GHz (radio contours are obtained from <http://skyview.gsfc.nasa.gov/cgi-bin/query.pl>). The western diffuse emission is well correlated with the radio emission.

The flux values of the spectra shown in Figure 2 are obtained by normalizing them with respect to $H\alpha$ flux value. With these flux values and taking the electron temperature at $\sim 10^4 K$, some basic parameters of SNR G85.9-0.6 are calculated and listed in Table 4. The fluxes corrected for interstellar extinction are normalized to $I(H\alpha) = 100$. For three region, $[SII]/H\alpha$, $[SII]\lambda\lambda 6716/6731$, $[OIII]/H\beta$ ratios and the parameters that are obtained from these ratios found to be comparable. The average values are considered while discussing the

results.

To find these parameters first, through [SII] $\lambda\lambda$ 6716/6731 flux ratio the electron density is calculated (Osterbrock 1989). Shock velocity is estimated from the ratio of [OIII]/H β as described by (Cox & Raymond 1985; Raymond et al. 1988; Hartigan et al. 1987).

Assuming that the remnant is still in the adiabatic phase of its evolution, the pre-shock cloud density n_c can be calculated by using the relationship $n[\text{SII}] = 45n_c (Vs/100)^2 \text{ cm}^{-3}$ (Dopita 1979; Fesen & Kirshner 1980). Where $n[\text{SII}]$ is the density calculated using the [SII] emission line from the optical spectra. This equation is valid if the transverse magnetic field is sufficiently low such that the magnetic pressure does not dominate the post-shock pressure as is discussed by Dopita & Sutherland (1996).

Shock wave energy E is given by the equation $2 \times 10^{46} \beta^{-1} n_c (Vs/100)^2 r_s^3 \text{ ergs}$ (see e.g. McKee & Cowie 1975) where r_s is the radius of the shock wave. The factor β is approximately equal to 1 at the blast wave shock.

The interstellar extinction ($E(B - V)$), absorption (Av), and neutral hydrogen column density ($N(\text{HI})$) are calculated through the relations $E(B - V) = 0.664c$, $Av = 3.1 \times E(B - V)$ and $N(\text{HI}) = 5.4 \times 10^{21} \times E(B - V)$ (Kaler 1976), (Aller 1984) and (Predehl & Schmitt 1995). Where c is $1/0.331 \log[(H\alpha/H\beta)/3]$.

Furthermore, [SII]/H α ratio is also calculated from the spectrum. In this calculation, λ 6716 and λ 6731 doublet line fluxes of [SII] is used. This ratio, for three coordinates whose α and β are given in the Table 2, is calculated at its average value to 0.46.

4. Discussion and Conclusions

In this work, the imaging and spectroscopic observations of the central part ($13' \times 13'$) of the galactic supernova remnant G85.9-0.6 is observed for the first time in optical band. The images show diffuse emission structure. As seen from the Figures 1,3, the dominant emission extends from south-west to north. The diffuse emission centered at $\alpha = 20^h 59^m 00^s$, $\delta = 44^{\circ} 52' 50''$ that covers an area $6' \times 8'$ is very well correlated with radio emission (see Fig.4).

As seen from the Tablo 3, [SII]/H α ratios take values between 0.2-0.6. This ratio is $\sim 0.5, 0.6$ on the places where dominant diffuse emission comes indicating ionization of the shock heated gas resulted from collision. On the other hand, the ratio of $\sim 0.2-0.3$ on the places where emission is faint indicating that resulted emission originate from photoionization mechanism. [SII]/H α ratio obtained from imaging is at 0.42 which is in agreement with spectral measurements of 0.46. These values imply that diffuse emission of G85.9-0.6 may be associated with HII region.

From the spectra, we see the presence of H α , H β , [OIII] $\lambda 4959, \lambda 5007$, [NII] $\lambda 6548, \lambda 6584$ and [SII] $\lambda 6716, \lambda 6731$, in addition a weaker [OI] $\lambda 6300$ and [OIII] $\lambda 4363$ emission lines. The presence of [OI] $\lambda 6300$ line emission indicates that the emission is originating from shock heated gas. Theoretical models predict electron temperature through [OIII]J($\lambda 4959 + 5007 / \lambda 4363$)ratio. Since [OIII] $\lambda 4363$ emission line is very close to Hg I $\lambda 4358$, it is almost impossible to differentiate them (Osterbrock 1989). Therefore, the electron temperature (T) assumed to be $10^4 K$ in this work.

We detected a weak [OIII]/H β emission line ratio at 1.18 indicating an oxygen-deficient remnant. Theoretical models of Cox & Raymond (1985) and Hartigan et al. (1987) give that for shocks with complete recombination zones this value is ~ 6 , while this limit is exceeded in case of shocks with incomplete recombination zones (Raymond et al. 1988).

Our values measured from spectra indicates that complete recombination takes place at those regions. Therefore, considering our measurements and the theoretical models mentioned above we estimated the velocity of the shock to be 80 km s^{-1} .

Since the G85.9-0.6 lies in the region between the local and Perseus spiral arms, it has a reliable distance, of 5 kpc (Kothes et al. 2001). For this distance and $\theta = 24'$ we calculated shock radius (r_s) to be $\sim 17.4 \text{ pc}$. Explosion energy and hydrogen column density of the G85.9-0.9 for this radius and estimated shock velocity is calculated, to be $\sim 9.2 \times 10^{50} \text{ ergs}$ and $\sim 1.53 \times 10^{21} \text{ cm}^{-3}$ respectively. This much energy can be considered as the typical energy released from a supernova explosion.

Typical value of the sulfur line ratio $[\text{SII}](\lambda 6716/\lambda 6731)$ for SNRs should be close to 1.5 (Frank et al. 2002). This ratio is calculated to be 1.13 indicating low electron density which is calculated as 395 cm^{-3} for this region.

We note here that, providing rather long exposure times and examining its surrounding region will give more information about the morphology and angular size of the G85.9-0.6 in optical band. The images taken with different interference filters like $[\text{NII}]$, $[\text{OIII}]$ will give more information about the inhomogeneities and density variations of the medium.

Acknowledgments

We thank TUBITAK for its support in using RTT150 (Russian-Turkish 1.5-m telescope in Antalya) under project number 09ARTT150-454-0. A.S. is supported by TUBITAK Post-Doctoral Fellowship. This work is supported by the Akdeniz University Scientific Research Project Management and by TÜBİTAK under project code 106T310. The authors also acknowledge the support by Bogazici University Research Foundation via code number 06HB301.

REFERENCES

- Aller, L.H., 1984, *Physics of thermal gaseous nebulae*, D.Reidel Publishing, Company, University of Queensland Press, Australia, 1984.
- Bamba, A., Yokogawa, J., Sakano, M., Koyama, K., 2000, *PASJ*, 52, 259.
- Boumis, P., Mavromatakis, F., Paleologou, E.V., 2002, *A&A*, 385, 1042.
- Boumis, P., Xilouris, E. M., Alikakos, J., Christopoulou, P. E., Mavromatakis, F., Katsiyannis, A. C., Goudis, C. D., 2009, *A&A*, 199, 789.
- Cox, D. P. and Raymond, J. C., 1985, *ApJ*, 298, 651.
- Dopita, M. A., 1979, *ApJS*, 40, 455.
- Dopita, M. A. and Sutherland, R. S., 1996, *ApJS*, 102, 161.
- Dopita, M. A., 1997, *ApJ*, 485, L41.
- Dopita, M.A., Kewley, L.J., Heisler, C.A. and Sutherland, R. S., 2000, *ApJ*, 542, 224.
- Fesen, R. A. and Kirshner, R. P., 1980, *ApJ*, 242, 1023.
- Fesen, R.A., Winkler, F., Rathore, Y., Downes, R. A., Wallace, D., 1997, *AJ*, 113, 767.
- Fesen, R., Rudie, G., Hurford, A., Soto, A., 2008, *ApJS*, 174, 379.
- Frank, J., King, A. and Raine, D., 2002, *Accretion Power in Astrophysics*, Cambridge University Press, Cambridge, New York.
- Gök, F., Sezer, A., Aslan, Z., Aktekin, E., 2008, *Ap&SS*, 318, 207.
- Green, D.A., 2009, *A Catalogue of galactic Supernova Remnants*, 2009 March version, <http://www.mrao.cam.ac.uk/surveys/snrs>.

- Hamuy, M., Walker, A.R., Suntzeff, N.B., Gigoux, P. Heatcote, R. and Phillips, M.M., 1992, *PASP*, 104, 533.
- Hartigan, P., Raymond, J.C., Hartmann, L., Gigoux, P., 1987, *ApJ*, 316, 323.
- Jackson, M. S., Safi-Harb, S., Kothes, R., Foster, T., 2008, *ApJ*, 674, 936.
- Kaler, J.B., 1976, *ApJS*, 31, 517.
- Katsuda, S., Petre, R., Hwang, U., Yamaguchi, H., Mori, K., Tsunemi, H., 2009, *PASJ*, 61, 155.
- Kewley, L.J., Dopita, M.A., Sutherland, R. S., Heisler, C.A. and Trevena, J., 2001, *ApJ*, 556, 121.
- Kothes, R., Landecker, T.L., Foster, T. and Leahy, D.A., 2001, *A&A*, 376, 641.
- Massey, P., 1997, *A User's Guide to CCD Reductions with IRAF*, 370, <http://iraf.noao.edu>.
- Mathewson, D. S. and Clarke, J. N., 1972, *ApJ*, 178, L105.
- Mavromatakis, F., Papamastorakis, J., Ventura, J., Becker, W., Paleologou, E. V., Schaudel, D., 2001, *A&A*, 370, 265.
- Mavromatakis, F., 2003, *A&A*, 398, 153.
- McKee, C.F. and Cowie, L.L., 1975, *ApJ*, 195, 715.
- Osterbrock, L.H., *Astrophysics of Gaseous Nebulae and Active Galactic Nuclei.*, 1989, California University Press, California.
- Predehl, P. and Schmitt, J.H.M.M., 1995, *A&A*, 293, 889.
- Raymond, J.C., 1979, *ApJS*, 39, 1.

Raymond, J.C., Hester, J.J., Cox, D., Blair, W.P., Fesen, R.A. and Gull, T.R., 1988, ApJS, 324, 869.

Shull, J.M. and McKee, C.F., 1979, ApJ, 227, 131.

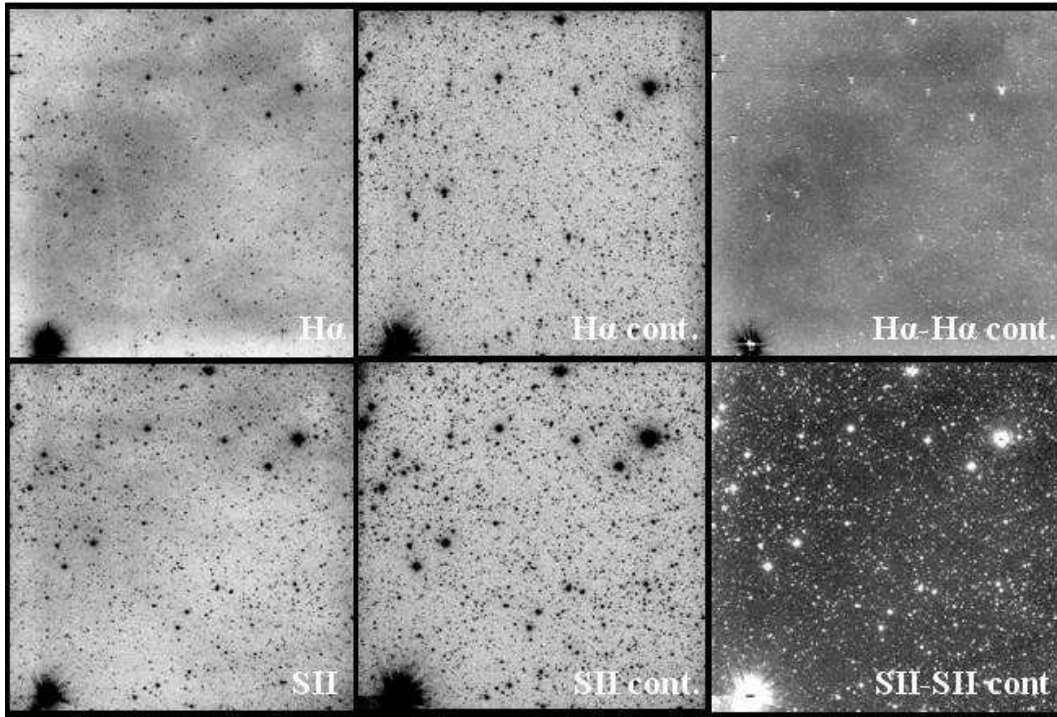


Fig. 1.— H α , H α cont., H α -H α cont., [SII], [SII] cont. and [SII]-[SII] cont. images of G85.9-0.6. Each field of view is 13.5 arcmin x 13.5 arcmin

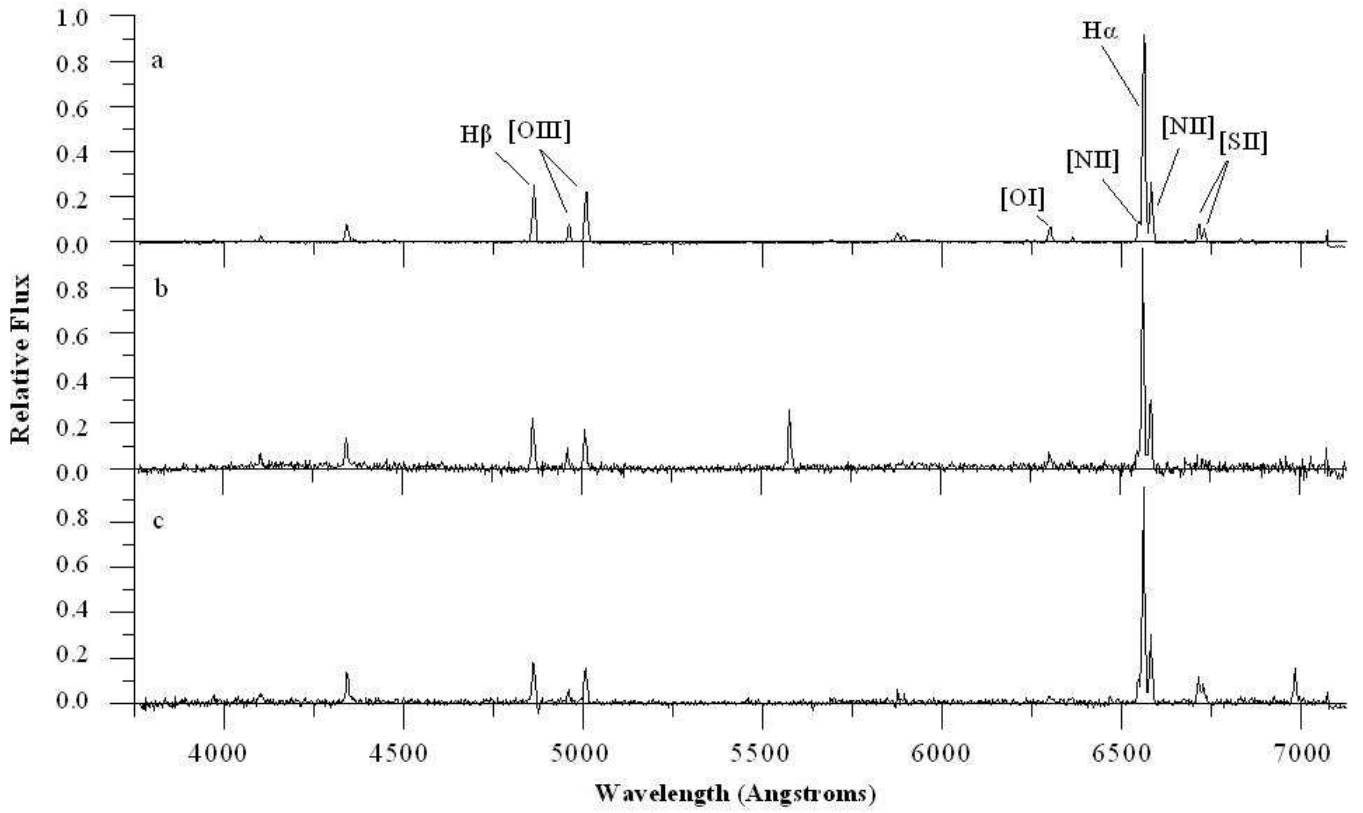


Fig. 2.— The long slit spectra of G85.9-0.6 for area 1 (a), area 2 (b) and area 3 (c)

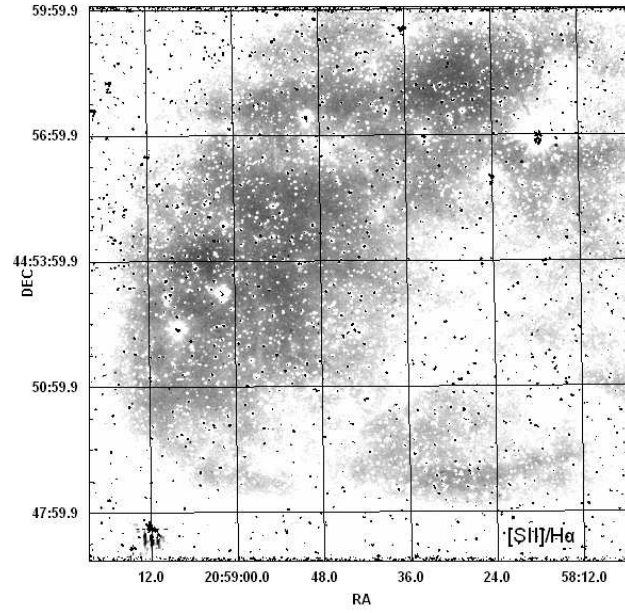


Fig. 3.— The negative of the $[\text{SII}]/\text{H}\alpha$ image of G85.9-0.6. The image has been smoothed to suppress the residuals from the imperfect continuum subtraction. Field of view is 13.5 arcmin x 13.5 arcmin

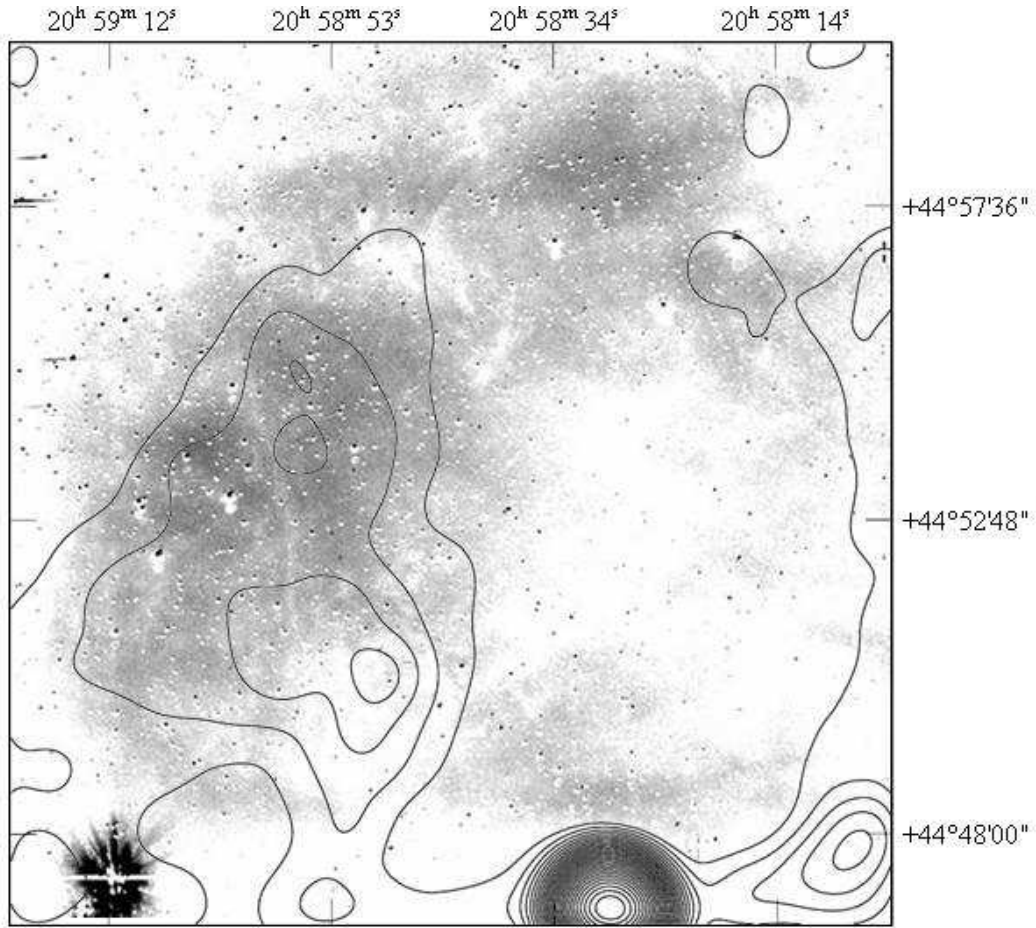


Fig. 4.— NVSS 1.4-GHz VLA radio continuum map superposed on the continuum subtracted and smoothed $H\alpha$ image of G85.9-0.6

Table 1: The journal of observations.

Filter	Wavelength (FWHM) (\AA)	Obs. Date (UT)	Exp. times (s)
H α	6563 (88)	01 June 2009	900
H α cont.	6446 (130)	01 June 2009	900
SII	6728 (70)	01 June 2009	900
SII cont.	6964 (300)	01 June 2009	900

Table 2: The spectroscopic observations.

Area	Slit Center (J2000)	Exposure times (s)
1	$\alpha = 20^h59^m04^s$ $\delta = 44^{\circ}52'19''$	600
2	$\alpha = 20^h58^m49^s$ $\delta = 44^{\circ}55'32''$	600
3	$\alpha = 20^h58^m32^s$ $\delta = 44^{\circ}58'24''$	600

Table 3: [SII]/H α ratios and their errors for different regions of the G85.9-0.6.

Area	coordinate J(2000) α , δ	[SII]/H α
1	20 ^h 58 ^m 29 ^s , 44 ^o 58'37"	0.6 (\pm 0.1)
2	20 ^h 58 ^m 33 ^s , 44 ^o 58'30"	0.5 (\pm 0.1)
3	20 ^h 58 ^m 49 ^s , 44 ^o 55'07"	0.5 (\pm 0.1)
4	20 ^h 58 ^m 53 ^s , 44 ^o 53'27"	0.5 (\pm 0.1)
5	20 ^h 58 ^m 48 ^s , 44 ^o 55'20"	0.4 (\pm 0.1)
6	20 ^h 58 ^m 29 ^s , 44 ^o 48'20"	0.3 (\pm 0.1)
7	20 ^h 58 ^m 18 ^s , 44 ^o 56'02"	0.3 (\pm 0.1)
8	20 ^h 58 ^m 11 ^s , 44 ^o 51'17"	0.2 (\pm 0.1)
9	20 ^h 59 ^m 03 ^s , 44 ^o 57'29"	0.3 (\pm 0.1)
10	20 ^h 59 ^m 04 ^s , 44 ^o 53'53"	0.6 (\pm 0.1)

Table 4: This table gives the relative line fluxes and the parameters obtained from spectra for three different areas of the G85.9-0.6. (F) shows fluxes uncorrected for interstellar extinction, (I) shows fluxes corrected for interstellar extinction. Numbers in parentheses represent the signal-to-noise ratio of the quoted values. All fluxes normalized $F(H_\alpha)=100$ and $I(H_\alpha)=100$. The errors of the emission line ratios and other parameters are calculated through standard error calculation.

Lines (\AA)	Flux ($F(H_\alpha)=100, I(H_\alpha)=100$)						Parameters	Values		
	Area 1		Area 2		Area 3			Area 1	Area 2	Area3
	F	I(S/N)	F	I(S/N)	F	I(S/N)				
4861 $H\beta$	28	52(58)	25	48(14)	20	34(26)	[SII]/ $H\alpha$	0.44 ± 0.01	0.45 ± 0.01	0.50 ± 0.09
4959 [OIII]	8	15(40)	11	21(7)	8	13(9)	[SII] λ 6716/6731	1.09 ± 0.08	1.14 ± 0.03	1.17 ± 0.2
5007 [OIII]	24	44(54)	19	35(10)	18	29(23)	[OIII]/ $H\beta$	1.14 ± 0.14	1.16 ± 0.20	1.23 ± 0.16
6300 [OI]	7	17(28)	9	13(4)	5	6(4)	Ne (cm^{-3})	470 ± 120	380 ± 40	336 ± 26
6548[NII]	10	10(28)	10	11(5)	13	14(11)	n_c (cm^{-3})	16 ± 3	13 ± 1	12 ± 1
6563 $H\alpha$	100	100(245)	100	100 (30)	100	100(124)	c	0.23 ± 0.02	0.38 ± 0.04	0.67 ± 0.07
6584[NII]	29	33(56)	33	31(9)	33	32(31)	E(B-V)	0.15 ± 0.02	0.25 ± 0.03	0.45 ± 0.05
6716 [SII]	25	23(40)	24	24(8)	23	27(7)	Av	0.47 ± 0.05	1.18 ± 0.12	1.40 ± 0.14
6731 [SII]	20	21(35)	20	21(7)	19	23(4)				